A novel method for increasing the wind turbine power by installing an optimized curved flange and a vortex generator on the shroud and investigation of entropy generation for shroud internal flow

Ali Niknahad
Amir Khoshnevis (khoshnevis@hsu.ac.ir)

Research Article

Keywords: flange, wind turbine, optimization, entropy, CFD

Posted Date: April 18th, 2022

DOI: https://doi.org/10.21203/rs.3.rs-1562419/v1

Abstract

In urban areas, the quality of the passing wind is low and it is not able to create the necessary force for the proper rotation of wind turbines. In the present study, a wind turbine is located in a shroud equipped with a straight vertical flange. The curvature of this vertical flange is constantly changed to create different curves. By using this procedure, a flange with an optimal curve that is able to create the highest mean velocity of air passing through the shroud will be obtained. Then, a circular vortex generator was installed on the body of the shroud, which can increase the airflow velocity through the shroud. The results have been confirmed by studies of turbulence kinetic energy behind the turbine shroud. Using the results of the three- dimensional simulation, important parameters of the turbine including power factor for different cases have been studied. To investigate the effect of using these innovations on the dissipation of flow energy, a study has been performed on the generated entropy of the flow passing through the shroud. The results show that the use of these tools has little effect on increasing entropy and therefore energy dissipation does not change significantly.

1 Introduction

The use of clean energy guarantees the health of the planet and future generations. The use of renewable energy, in addition to reducing pollution from fossil fuels to generate power, will preserve fossil fuel reserves for the future. In the meantime, wind turbines and related equipment have a wide position, but it is necessary to pay attention to the fact that they must be built with the best design and then reach the consumers. The use of novel and optimal aerodynamic shapes has always resulted in lower costs and higher efficiency. Therefore, aerodynamic optimization and novel design are very necessary for the construction of wind turbine shrouds, which are an integral part of urban wind turbines. In the following, past works related to the aerokinetic and hydrokinetic turbine shrouds will be examined in order to create a necessary background for the present work.

Changing shroud's original geometry and using new designs to build different geometries is one of the efficient designers' point of view on wind energy. Humans are expanding their use of wind energy in the current context in which the growing need for energy is clearly felt. The total manufacture in 15 nation state in Western Europe is extremely connected and it is exposed that the total -production is conquered by a digit of main mechanisms far less than the sum of nations. This establishes the connection of wind power construction in the greater zone, Ahlborn, Detlef [1]. The shrouds of power generation turbines, due to their importance in increasing power, have been studied experimentally and numerically in various works. Shroud geometries are assessed for their amplification of flow velocity over the turbine. Early investigations are done by means of axisymmetric computations of annular wings with high-lift airfoils as cross sectors. The flow velocity strengthening parameter is proposed as an operating, Aranake et al. [2]. An axisymmetric RANS solver is used with an actuator disk model for the examination of shrouded wind turbine flow fields. The optimum result is also assessed using a full 3-D RANS solver. Instead of assessing the forces based on a given blade twist, the blade twist is defined such that the angle of attack of each segment is optimum regarding the local flow angle, Aranake and Duraisamy [3]. The diffuser shroud mechanism can draw the airflow over buildings to guide and accelerate the airflow inside. The CFD result approves the functionality of

the fluid machine to take advantage of the airflow over buildings for wind power generation. Power amplification using a diffuser and shrouded edges around conventional wind turbines shows a noteworthy power coefficient increase, Dilimulati et al. [4]. Assessing hydrokinetic turbines in yaw conditions contributes to approximating turbine performance, power constancy, and power carried to the network. Water tunnel tests show the performance reduction using three strategies: no shroud, a convergent-divergent shroud, and a diffuser shroud. Experimental outcomes demonstrate that the output power decreases in off-axis flows for all strategies studied. Off-axis operations also reduce the operating range of a turbine, Shahsavarifard and Bibeau [5]. A half-opened duct surpasses the normal shrouds in power and rotor speeds in higher ranges of wind velocity. Using the proposed apparatus can cut drag force on the duct construction beside the turbine functionality, Siavash et al. [6].

Adding some tools to the turbine and shroud system will further increase the production capacity of the turbine. In this field, we can name stators, lobed ejectors, diffusers, etc. By using pre-swirl stators to the shroud, it is possible to change the inlet flow in order to maximize net tangential force on the turbine blades and grow power output. Four dissimilar pre-swirl stator arrangements were planned and examined on a shrouded 3-bladed turbine, Gish et al. [7]. Modeling outcomes showed that the wind energy application productivity of the suggested wind turbine amplified at low wind velocities. The shroud and lobed ejector construction in the rear of the suggested turbine created such an upshot that the pressure at the turbine outlet was reduced with the purpose of increasing the turbine power output, Han et al. [8]. The functionality augmentation is influenced by numerous factors such as the diffuser geometries, blade airfoils, and the wind condition at the mounting site. Adding a simple conical diffuser can augment the micro wind turbine coefficient of functionality by using a nozzle conical diffuser shroud compared to the simple turbine. The diffuser and nozzle-diffuser grow optimum TSR compared to the simple turbine, Kosasih and Tondelli [9]. By adding a diffuser to the system, the turbine power generation increases. A diffuser without an inlet shroud is capable to augment wind velocity up to 10% but a diffuser with an inlet shroud can augment wind velocity only up to 13.3%. Wind turbines without a diffuser's power efficiency is 11.2%, and diffuser without an inlet shroud has a power efficiency of 13.5% and also a power growth of 20.5%. The diffuser with the inlet shroud has a maximum power efficiency of 15.8% so the diffuser with the inlet shroud is able to grow power efficiency by 41.1%, Pambudi et al. [10].

Optimizing and modifying the shroud and flange geometry are also two of the things that are very important in increasing the production capacity of the turbine. The improvement of a modular optimization pattern for the aerodynamic form optimization of diffuser-amplified wind turbine shrouds is reported. For the numerical modeling of the stream domain, an axisymmetric RANS solver has been applied. The basis of the optimization structure is shaped by a parallel and asynchronous Differential Evolution algorithm, Leloudas et al. [11]. A modified shroud profile (SD2) was shaped by thickening SD1. The aerodynamic functionality of SD2 was not far poorer. Furthermore, a noteworthy volume drop for SD1 and SD2 was reached. Both SD1 and SD2 caused meaningfully minor flow separations near the outlet surface, which is recognized as the chief reason for the growth in acceleration and drag-drop, Leloudas et al. [12]. The extraordinary growth in wind speed is obtained. The best shape of the flanged diffuser in order to find a greater power production of the shrouded wind turbine is examined. A flanged diffuser-shrouded wind turbine established power amplification compared to a bare wind turbine. The flange also works like a rudder and the shrouded wind

turbine always faces in the direction of the upcoming wind, Ohya et al. [13]. The mathematical model exposed that any shroud with an optimum design barely can offer a CP = 1 for a wind turbine. The model exposed that the speed-up ratio has an optimum value that is governed by absorbed energy by the rotor and duct, Siavash et al. [14]. A lower-order model for forecasting the functionality of shrouded wind turbines for a range of shroud airfoil shapes was provided. Great engineering estimates can be obtained by using the algebraic solutions of this technique. To get better results from this model, there are some aspects of the model that must be considered before beginning the shrouded turbine design, Werle [15].

In some cases, changing the arrangement of the turbine and adding additional rotor can have a positive effect on system performance. While boosting the wind turbine functionality, shrouding growths meaningfully the rotor loading. A cure for it is the application of another rotor. Although it offers an efficiency increase, it permits loads to be spread more uniformly on turbines. After using shrouding, an around double growth in the first wind turbine power coefficient has been seen at the identical wind velocity. By using the two-rotor system, it has been probable to decrease the thrust coefficient of the first turbine and reduce the optimal TSR, Lipian et al. [16]. The outcomes of URANS modeling for different arrangements of single and twin-rotor, bare, and shrouded machines are assessed. The existence of the second rotor could decrease the mass flow rate through the first wind turbine, Lipian et al. [17].

Calculating the generated entropy in aerodynamic structures and controlling it is one of the important principles in aerodynamic designs. Flow separation has an extreme consequence on viscous entropy production rate. The raises of the separation part of airfoil in the higher AOA create more entropy because of the higher shear layer section. Furthermore, a relation between entropy production integral and drag coefficient exists, Mamouri et al. [18]. An airfoil is modified based upon the entropy examination results. Later, the unsteady aerodynamic factors modified airfoil will be studied. The results display that a more appropriate airfoil might be elected based upon the wind turbine's revolution frequency, Mamouri et al. [19].

In the meantime, one can be inspired by the tools used in other aerial structures such as airplanes. One of these tools is vortex generators. This tool has also been used in the present study. An assessment was done among circular and triangular vortex generators on the wing of Boeing-737. Moreover, the average velocity and instable velocity components in the wake area are examined by CFD, Niknahad and Khoshnevis [20].

Due to the increasing need of households for energy, newer methods should be used to increase the production capacity of wind turbines. This need can create a gap that has been tried to fill in the present work. Also, the use of optimization methods, efficient and at the same time simple geometries to increase the power of urban wind turbines is an important matter that has been given special attention in the present work.

In the present study, by using two-dimensional optimization of a vertical straight flange installed on an urban wind turbine, an aerodynamic curve-shaped flange with the ability to create the maximum wind mean velocity passing through the shroud has been obtained for the first time. Then the values are confirmed by examining the results of turbulence kinetic energy. Also, in order to further increase the turbine power, a circular vortex generator has been installed on the outer body of the shroud for the first time. With the results obtained from the three-dimensional solution of shrouds with simple and shrouds with optimal curved

flanges and with and without circular vortex generator, the changes in mean velocity at the inlet and outlet of the shroud, torque on the blades, the rotational velocity of the blades, and turbine power coefficient and also the drag force on each entire shroud structures is calculated and described. Also, entropy generation due to viscous effects of shroud internal flow has been studied.

2 Methodology

In this paper, as the first innovation, many wind turbine shroud flange curvatures in order to find the optimum geometry for catching and accelerating the wind, are investigated. The flow around two-dimensional wind turbine shrouds is solved by considering the unsteady characteristics of the flow around it. For considering the turbulent nature of the flow field, RSM turbulent model is found well and used for flow simulation. Finally, the flow field variables in each case are compared to find the optimum wind turbine shroud flange curvature based on which design can maximize the shroud inlet mean velocity after time-averaged flow variables had reached an unchanging state with time passing. As a second innovation, a circular vortex generator is installed on the outer body of the shroud, which can further increase the speed of the air passing through the shroud. After this step, the accuracy of the results obtained from the two-dimensional solution is evaluated using three-dimensional simulation results. Also, the drag force on the whole structure in different designs has been calculated and compared. In the next step, using the results obtained from the three-dimensional solution with a sliding grid, the effect of this increase in air velocity on the aerodynamic forces on the turbine blades, turbine output torque, turbine rotational speed, and power coefficient of the turbine is investigated. Finally, by examining the results of the three-dimensional solution, the entropy changes of the airflow through the shroud in different cases are investigated and also compared.

2.1. Governing equations

In this study, the airflow Mach number is below 0.3 and the assumption of incompressibility is valid. Thus the incompressible form of continuity, momentum, and energy equations for turbulent flow is considered. The method used for considering the turbulent nature of the flow field is implementing the RANS equitation for governing equations and RSM turbulent model. Equations 1 to 3 show the RANS form of continuity, momentum, and energy equations, respectively. Also, dissipation due to friction and Reynolds stress is considered by implementing the dissipation function $\varnothing$ in the energy equation. The important point in the entropy calculations given in this section is that in the energy equation dissipation term, perturbation parameters are also considered and therefore it is a good indicator of the effect of perturbations on flow energy dissipation. The results of the energy equation are used to obtain the domain entropy.

$$\frac{\partial \bar{u}}{\partial x}+\frac{\partial \bar{v}}{\partial y}=0 \tag{1}$$

$$\bar{u}\frac{\partial \bar{u}}{\partial x}+\bar{v}\frac{\partial \bar{u}}{\partial y}+\frac{1}{\rho}\frac{\partial \bar{p}}{\partial x}=\nu(\nabla^2\bar{u})-\frac{\partial \overline{(u')^2}}{\partial x}-\frac{\partial \overline{(u'v')}}{\partial x} \tag{2}$$

$$\frac{\partial \rho \bar{H}}{\partial t} + \frac{\partial}{\partial x_j}\left[\rho \bar{u}_j \bar{H} + \rho \overline{u_j' H'} - k\frac{\partial \bar{T}}{\partial x_j}\right] = \frac{\partial \bar{p}}{\partial t} + \frac{\partial}{\partial x_j}\left[\mu \bar{u}_i \left[\frac{\bar{u}_j}{\partial x_i} + \frac{\bar{u}_i}{\partial x_j}\right] + \mu\left[\overline{u_i' \frac{u_j'}{\partial x_i}} + \overline{u_i' \frac{u_i'}{\partial x_j}}\right]\right] \quad (3)$$

Where $\bar{u}$ and $\bar{v}$ are the mean velocities in the horizontal and vertical directions, respectively. $\bar{p}$ and ρ are also mean pressure and density, respectively. Also ν is kinematic viscosity. $\bar{H}$ stands for enthalpy and $\bar{T}$ stands for temperature. The prime symbol on each quantity indicates the oscillation value of that quantity.

2.2. Turbulent model

For considering the turbulence nature of the flow field, second-moment closure Reynolds stress model (RSM) turbulence modeling is used. RSM relies on the “Reynolds Stress Transport Equation” and equations 4 to 13 show all employed equations in the corresponding model. The equation for the transport of kinematic Reynolds stress $R_{ij} = \langle u_i' u_j' \rangle$ is:

$$\frac{DR_{ij}}{Dt} = D_{ij} + P_{ij} + \Pi_{ij} + \Omega_{ij} - \epsilon_{ij} \quad (4)$$

Production term:

$$P_{ij} = -\left(R_{im}\frac{\partial u_j}{\partial x_m}\right) + R_{im}\frac{\partial u_i}{\partial x_m} \quad (5)$$

Rapid pressure-strain correlation term:

$$\frac{\Pi_{ij}^R}{k} = C_2 S_{ij} + C_3\left(b_{ik}S_{jk} + b_{jk}S_{ik} - \frac{2}{3}b_{mn}S_{mn}\delta_{ij}\right) + C_4(b_{ik}W_{jk} + b_{jk} + W_{ik}) \quad (6)$$

$$b_{ij} = \frac{\bar{u_i}u_j}{2k} - \frac{\delta_{ij}}{3} \quad (7)$$

Slow pressure-strain correlation term:

$$\Pi_{ij}^{S} = -C_1 \frac{\epsilon}{k}\left(R_{ij} - \frac{2}{3}k\delta_{ij}\right) - C_2\left(P_{ij} - \frac{2}{3}P\delta_{ij}\right) \quad (8)$$

Dissipation term:

$$\epsilon_{ij} = \frac{2}{3}\epsilon\delta_{ij} or e_{ij} = 0 \quad (9)$$

$$e_{ij} = \frac{\epsilon_{ij}}{\epsilon} - \frac{2\delta_{ij}}{3} \quad (10)$$

Diffusion term:

$$D_{ij} = \frac{\partial}{\partial x_m}\left(\frac{v_t}{\sigma_k}\frac{\partial R_{ij}}{\partial x_m}\right) = div\left(\frac{v_t}{\sigma_k}\nabla\left(R_{ij}\right)\right) \quad (11)$$

$$v_t = C_\mu \frac{k^2}{\epsilon}, \sigma_k = 1, C_\mu = 0.090 \quad (12)$$

Rotational term:

$$\Omega_{ij} = -2\omega_k\left(R_{jm}e_{ikm} + R_{im}e_{jkm}\right) \quad (13)$$

$e_{jkm} = 1$, if i, j, k are in cyclic order and are different. $e_{jkm} = -1$, if i, j, k are in anti-cyclic order and are different. $e_{jkm} = 0$ in case any two indices are the same.

2.3 Entropy equation

Yadegari and Khoshnevis [21] used Eq. 14 to calculate the entropy production rate. In this equation Sg is the volumetric entropy production rate, T0 is the reference temperature, φ is entropy production rate by viscosity, and ϕ_θ is entropy production rate by heat transfer.

$$S_g = \frac{\bar{\phi}}{T_0} + \frac{\bar{\phi}_\theta}{T_0^2} \quad (14)$$

Viscous dissipation consists of two terms, $S_{g,\upsilon}$ and $S_{g,T}$.

$$\frac{\bar{\phi}}{T_0} = S_{g,\upsilon} + S_{g,T} \quad (15)$$

Where $S_{g,\upsilon}$ is the entropy production rate due to the mean flow dissipation and $S_{g,T}$ is the entropy production rate due to the dissipation of velocity fluctuations.

2.3. Geometry

Shown in Fig. 1 is a three-dimensional schematic of the shroud with vortex generator and flange attached to its end. In this figure, the perspective view and the side view are shown to better understand the system in the present study. Due to this geometry and its symmetry and according to previous researches, two-dimensional geometries can be used to perform the optimization process. In the present study, unlike many previous works and based on Gish et al. [7], NACA 0006 airfoil has been used in the design of shroud cross-section in two-dimensional and three-dimensional simulations, which can increase the output power. The diameter of the shroud inlet is considered to be 302.24 mm. Also, the length of the shroud based on Ohya et al. [13] is obtained using the ratio L/D = 1.5, hence the length of the airfoil chord is considered to be 450 mm. A vertical straight flange is installed at the end of the shroud, which is also known as a simple straight flange. Also, the value of flange height is obtained based on the relationship h/D = 0.25 according to Ohya et al. [13]. As mentioned earlier, one aim of the present study is to find an optimal aerodynamic shape for the flange. The curvature of the vertical flange is constantly changed at very short intervals to achieve an optimal curvature angle and creates a special curve at each step. For this purpose, by moving the center point of the flange towards the shroud outlet with very small values, flanges with different curves are obtained. In this way, a wide variety of shapes of the flange are obtained. For the sake of brevity, in this article, only five of these cases have been examined for an explanation. A schematic of the two-dimensional shroud geometry with straight-vertical flange (case1) and flanges with angles of curvature (δ) of 1.518 degrees (case 2), 14.840 degrees (case3), 27.920 degrees (case 4), and 33.521 degrees (case 5) is shown in Fig. 2. To further increase the speed of the air passing through the shroud, a circular vortex generator is installed in the middle of the

outer wall of the shroud according to Niknahad and Khoshnevis [21]. The diameter of the circular vortex generator is 22.5 mm and its center is 201.135 mm from the entrance of the shroud and is located right in the middle of the shroud chord. In this research, a three-bladed turbine with 5 degrees pitch from root to tip has been used. The airfoil SG6040 is used for the turbine root and SG6043 for the turbine root. The length of each blade is equal to 150 mm and the diameter of the hub is equal to 50 mm and its length is equal to 60 mm. Details are shown in Fig. 1.

2.4. Grid generating and mesh independency

In this section, meshing and examining the mesh independency for two-dimensional and three-dimensional studies are discussed in turn. To check the mesh independency, using the maximum or minimum values of the flow parameters in the computational domain give better results than the average values. Therefore, in this study, the maximum values of mean velocity and turbulence kinetic energy are presented to investigate mesh independency. After reviewing the results obtained from meshing with different sizes, the optimal mesh size for two-dimensional and three-dimensional simulations has been selected.

Table 1 Grid independency for two- and three-dimensional simulations

Model dimension	Grid cell number	Max mean velocity of domain(m/s)	Max k of domain(m^2/s^2)
2-D	178,390	16.800	30.526
	267,590	18.480	33.579
	401,380	20.328	36.937
	602,100	20.348	36.973
3-D	1,394,000	23.798	19.332
	2,091,000	26.178	21.265
	3,167,000	28.795	23.392
	4,705,000	31.675	23.415
	7,058,000	34.843	25.756
	10,587,000	34.876	25.781

According to the observations from Table 1, the number of optimal grid cells for two and three-dimensional geometries is 602,100 and 7,058,000, respectively. The reason for selecting this number of grid cells is that the changes in flow parameters are less than 0.1%. Also, to study the effect of wind velocity on the rotation of turbine blades, a sliding grid around the turbine blades has been used, which makes it possible to calculate the rotational speed and power coefficient. The gridding used in this research uses the Tet / Hybrid element and is TGrid type. Figure 3(a) and 3(b) and 3(c) show the mesh grids used in 2D and 3D simulations, respectively, based on the results of mesh independency.

In this section, in addition to examining the mesh independency, the Y + diagram is also examined. What comes out of Fig. 4 is that the amount of Y + is much less than unity around the shroud so the mesh grid can be considered acceptable.

2.5. Numerical method

In this study, the corresponding governing equations are solved numerically with ANSYS 18.1 solver with double-precision accuracy and pressure-based algorithm, and Semi-Implicit Method for Pressure Linked Equations is selected as the appropriate pressure-velocity coupling. For capturing the time-dependent characteristics of the fluid flow field, the unsteady terms in equations are considered. The second-order accuracy for all discretization of governing equations is selected in order to ensure sufficient accuracy. The convergence criterion is selected 10^{-5} for error between iterations of equations except for the energy equation. The value of 10 − 8 is selected for the energy equation.

2.6. Boundary condition

In order to simulate the flow in and around the wind turbine shroud, we assume that an inlet with velocity inlet condition is used which enters the air into the computing domain at 15 meters per second. Considering laminar free stream, the inlet turbulent intensity in this research is considered equal to 0.1%. The output of the computational domain is selected as outflow, which has a good accuracy due to the fact that the flow is developing. This statement has been proved by comparing the results with previous works during simulation. Turbine blades have a no-slip boundary condition.

3 Results And Discussion

3.1. Validation

The validity of the proposed numerical method is confirmed by comparing the numerical simulation with the experimental results of Ohya et al. [13]. Ohya et al. [13] conducted a wind tunnel experiment to obtain the pressure coefficient and mean velocity distribution inside three different types of shroud. One of these shrouds is a diffuser type that expands its cross-sectional area left to right similar to the present study. In their experiment, a diffuser with a square section with a side length of 0.4 m and with a half-open angle of 4 degrees was used. At the trailing edge of the shroud, a ring-type square flange with h/D = 0.25 is installed. The discussed apparatus was then placed in a boundary-layer type wind tunnel and the approaching wind velocity is set as 5 m/s. Figure 5 shows the explained diffuser type shroud.

Ohya’s experiment results were reproduced with the proposed numerical method in the present study and these results are compared with corresponding Ohya’s results, as shown in Fig. 6. The comparison confirmed that there is good agreement with experimental results and numerical methods. The average error between the turbulence model and the method used in this research and experimental work is less than 10%. The small difference between results is because of the two-dimensional simulation of the geometry used in Ohya’s experiment.

3.2. Determining the optimum curvature

The results for determining the optimum curvature for the installed flange are presented. In this study, the straight vertical flange is exposed to bending. Various curvatures are examined to find the optimum curvature that produced the maximum mean velocity within the wind turbine shroud. To summarize the results, only five studied cases are presented here. Figure. 7 shows the mean velocity profiles at the inlet of the shroud with straight vertical flange (case 1) and shrouds with carved flanges with curvature angles of 1.518 degrees (case 2), 14.840 degrees (case 3), 27.920 degrees (case 4) and 33.521 degrees (case 5). The inlet flow mean velocity continues to increase until reaching maxima and then due to over bending of the flange, the inlet mean velocity starts to decrease. The non-dimensional mean velocity magnitude throughout of inlet section of case 4 is higher than the others. This figure expresses that the effect of flange curvature on shroud internal flow is to increase the internal flow mean velocity. It should be noted that these results are based solely on the design performed on the flange and numerical uncertainty has no role in these results.

Table 2 shows the average non-dimensional inlet mean velocity for all cases. This must be kept in mind that according to Leloudas et al. [11], these models are two-dimensionally simulated but the changing trend can be cited acceptably.

Table 2 The values of average non-dimensional inlet mean velocity and its increase percentage for cases 1–5

Case number	Average mean u/U0	Increase percentage
Case 1	1.558	-
Case 2	1.563	0.320%
Case 3	1.582	1.540%
Case 4	1.587	2.850%
Case 5	1.565	0.449%

Figure 9 shows the mean velocity profile just behind the shroud for cases 1 to 5. Figure 8 shows the two-dimensional shroud and the station behind it, where the average velocities are measured in this section.

In Fig. 9, it is clear that for case 4, severe vortices occur at the station shown in Fig. 8, around the flange, resulting from the very intense vortices created by case 4. These vortices are exactly the same vortices that create a low-pressure area behind the shroud and consequently increase the mean velocity of air passing through the shroud. The other four geometries, due to the aerodynamic form of their flange, almost have similar and monotonous profile shapes.

Figure10 shows the velocity contour of a three-dimensional geometry cross section with numerical values of the contour. What is clear in this figure is that the velocity along the shroud, while using an optimal curved flange and an circular circular vortex, is higher than when the shroud is equipped with only a vertical straight flange. Behind of the shroud, in the case of an optimal curved flange and a circular vortex generator are used

on the shroud, stronger vortices can be seen than the shroud with a simple flange. Based on the results of this contour, it is proved that changing the geometry of the flange from vertical to curved with a suitable angle of curvature and using a circular vortex generator will have a positive effect on increasing the air flow through the shroud.

Figure 11 (a) shows non-dimensional mean velocity behind shroud ,at the station shown in Fig. 8, for cases 1 to 5. The vertical axis in this image is the ratio of the non-dimensional mean velocity over the entire area behind the shroud. Accordingly, the highest value is for case 4. Also, the increase in entry mean velocity to the shroud can be examined from the perspective of the average turbulence kinetic energy at the stations behind the shroud. The flanges installed at the end of the shroud create vortices that the deformation of the flange towards the optimal point increases the strength of these vortices. Therefore, the amount of turbulence caused by vortices should also be increased. Figure 11 (b) shows non-dimensional average turbulence kinetic energy behind the shroud, at the station shown in Fig. 8. From this figure, it follows that by examining different cases, by moving towards the flange with the optimal curved shape, the amount of turbulence kinetic energy will also increase and after passing this point, it will start a decreasing process. This finding agrees with the results obtained from the mean velocity survey section at the shroud entrance.

3.3. Comparison of the 3D shroud with optimal curved flange and circular vortex generator performance with the functionality of vertical straight flange shroud

In this section, the results obtained from the numerical simulation of a shroud equipped with a flange with an optimal curved shape, as the first innovation, and a shroud with a simple straight vertical flange are investigated. The purposes of presenting the results of this simulation are to compare the mean velocity in the part where the turbine is located, called the turbine part. Based on the preceding section results, it was found that the location of the turbine should be 118.8 mm away from the inlet of the turbine, the throat. Also, based on the suggestions presented in previous researches, the drag force on the whole shroud structure has been calculated and reported. Therefore, structural engineers can design and select the appropriate materials. In addition to using the optimal curved flange, another innovation that has been done in this work is the use of a circular vortex generator on the body of the shroud. This vortex generator creates a greater pressure difference between the inlet and outlet of the shroud. This greater pressure difference increases the flow of air through the shroud and increases the turbine power as well. Table 3 shows the non-dimensional average mean velocity at the turbine section and its increased percentage for shrouds equipped with optimal curved flange with and without vortex generator and that equipped only with vertical straight flange.

Table 3 The values of non-dimensional average mean velocity in the turbine section and its increase percentage for shroud with simple and optimum curved flanges with and without circular vortex generator

Models	u/U0	Increase percentage
Shroud + simple vertical flange	2.379	-
Shroud + optimal curved flange	2.470	3.825
Shroud + optimal curved flange + vortex generator	2.567	7.902

Therefore, based on the above results, it is obtained that the use of optimally curve-shaped flange can increase the airflow velocity ratio through the turbine section by 3.825%, and this is the first time that the flange deformation to an aerodynamic curved shape and optimization of it lead to an increase in mean velocity at the location of the turbine to this value. Another innovation that has been addressed in the present work is the use of circular vortex generators. According to the results obtained after connecting the vortex generator on the shroud, the speed ratio in the turbine section has increased to 2.567. This equates to a 7.902 percent increase in airflow velocity in the turbine section compared to when a shroud with a simple vertical flange is used. In this way, the vortex generator can be introduced as one of the new amplifying devices. Figure 12 shows the velocity contour at the turbine section for different situations. Figure 12 (a) shows the velocity contour around the turbine that has no shroud around it. Figure 12 (b) shows the velocity contour for a turbine in a shroud with an optimal curved flange equipped with a circular vortex generator. Figure 12 shows that with the use of new amplification methods, the velocity of the airflow in the turbine section grows, and consequently the rotation speed of the turbine blades increases. In Fig. 12 (a), the average velocity around the turbine blades is about 17 meters per second. In Fig. 12 (b), the velocity of airflow around the turbine is about 38 meters per second. By comparing this value with the amount of air velocity passing around the turbine without any shroud, it is obtained that the use of optimized curved flange and a circular vortex generator increases the air velocity passing around the turbine by 123.5%.

Based on the suggestions given in the works of the past, drag force information needed by structural engineers is provided. In this step, the total drag on the whole structure is examined. The results of this study can be useful in selecting the correct shape and materials for the construction of a wind turbine installation tower. Due to the strong pressure difference between the front and rear of the shroud, which is the main purpose of the present study, more drag force is applied to the shroud. This drag force is eventually transmitted to the turbine tower and this structure must have sufficient resistance to overcome the drag force. Table 4 shows the amount of drag on the shroud with a simple flange and the shroud with an optimal aerodynamic curved flange. The use of a curved flange with an optimal curved shape can increase the drag force applied to the shroud by 27.065%. Therefore, the use of stronger structures is required to build a turbine tower that can withstand this increase in drag force well when a shroud with a curved flange is used.

Table 4 The values of total drag force on shroud with simple and optimum curved flanges and its increase percentage

Models	Total drag force(kN)	Increase percentage
Shroud + simple vertical flange	30.400	-
Shroud + optimal curved flange	38.628	27.065

3.4. Effect of the curved flange and circular vortex generator on turbine angular velocity and turbine power factor

Creating a curve on the flange will increase the airflow through the shroud, which can create stronger aerodynamic forces on the turbine blades. In Table 5a comparison is made between turbines in a shroud with straight vertical flange, shroud with curved flange equipped with and without circular vortex generator, and also turbine without any shroud. Using a dynamic grid around the turbine, Table 5 presents the results of turbine torque and obtained angular velocity in different configurations as well as the corresponding power coefficient in the same wind velocity. The bare turbine is capable of producing a torque of 0.123 N.m, angular velocity of 138.005 rad/s, and power factor of 0.141 at wind speeds of 15 m/s. Using a shroud with a straight flange, the torque is increased by 156.097 percent to 0.315 N.m. The rotational velocity increases by 56.787% to 216.375 rad/s. Also, the power factor reaches 0.568, which indicates an increase of 302.836% compared to the turbine without a shroud configuration. Using the turbine in a shroud with optimal curved flange, the amount of torque, angular velocity, and power factor compared to turbines in a shroud with simple vertical flange has increased by 10.793%, 3.810%, and 15.140%, respectively. By installing a circular vortex generator these percentages will be equal to 14.285%, 7.937%, and 23.415%, respectively.

Table 5 Various specifications for different shroud models

Model	Total force(N)	Torque(N.m)	Obtained rotational velocity(rad/s)	Power coefficient	Increase of power coefficient relative to the bare turbine
Bare	1.257	0.123	138.005	0.141	-
Straight	3.09	0.315	216.375	0.568	302.836
Curved	3.330	0.349	224.620	0.654	363.829
Curved + VG	3.600	0.360	233.549	0.701	397.163

3.5. Investigation of entropy changes of shroud airflow by changing the structure of shroud geometry

In this section, the behavior of entropy changes with the structure of shroud geometry is investigated. The results of Table 6 indicate that by changing the structure of the shroud in such a way that the pressure difference between the front and back of the shroud increases and consequently the velocity of the air

passing through the shroud increases, the amount of flow entropy also increases. From this, it can be seen that increasing the airspeed in the shroud can increase the energy dissipation, which is the required energy that can be used to increase the power of the turbine. Therefore, researchers are expected to minimize this increase in entropy in future works by using materials that produce less friction and to enable the maximum extraction of available wind energy. However, the results show that the increase in entropy in the flow through the shroud is very small when a curved flange and a circular vortex generator are installed on the shroud and do not cause significant losses. The largest increase in entropy occurs when a curved flange and a circular vortex generator are used on the shroud, and this increase is only equal to 1.067%, which is a very small amount. Therefore, the use of these tools in the current situation is still very desirable. Following is a discussion of diffuser efficiency for shroud with a curved flange and a circular vortex generator. According to the literature, a well-designed diffuser efficiency should be between 90 and 95%. Efficiency of shroud introduced in the present work has a value equal to 94.8%. This efficiency is a confirmation on the excellent design of the shroud equipped with optimal curved flange and circular vortex generator.

Table 6 Average entropy in shroud when using shroud with different geometries

Model	Average entropy in the shroud (j/kg-k)	Increase percentage
Shroud + simple vertical flange	34.485	-
Shroud + optimal curved flange	34.508	0.066
Shroud + optimal curved flange + vortex generator	34.853	1.067

4 Conclusion

The present paper deals with the curvature optimization of the flange connected to the end of the wind turbine shrouds and the use of a circular vortex generator on the shroud body. For this purpose, the curvature of a vertical flange is constantly changed at very short intervals to achieve an optimal curvature angle and creates a special curve at each step. In this way, a wide variety of shapes of the flange are obtained. For the sake of brevity, in this article, only five of these cases have been examined for explanation. Then, by solving the governing equations of the flow field, the increase in mean velocity at the inlet of the shroud, torque on the blades, obtained rotational velocity of the blades, turbine power coefficient, and flow entropy generation in shroud have been studied.

- The results show that by curving the simple vertical flange of the shroud at the angle of 27.920 degrees, a curve is obtained that will be able to create the maximum mean velocity at the entrance and consequently along the entire length of the shroud.
- It is concluded that in the turbine section, a mean velocity increase of 3.852% can be achieved, which is the first time that using an aerodynamic curved cross-section for the flange of the shroud and optimizing it has achieved such a great increase in the air mean velocity along with wind turbine shroud.

By using a circular vortex generator on the body of the shroud, this amount of speed increase can be increased to 7.902%.

- The results show that curved flange sections continuously increase the turbulence kinetic energy of these areas compared to the case using a simple vertical flange until they reach the optimal shape. After passing the optimal point, the amount of turbulence kinetic energy in these areas decreases. This confirms past findings.
- Based on the aerodynamic calculations performed in the present study, the optimal aerodynamic curved flange can increase the amount of drag force applied on the shroud by 27.065%. These results can be used by structural engineers to design turbine towers.
- The bare turbine is capable of producing a torque of 0.123 N.m, angular velocity of 138.005 rad/s, and power factor of 0.141 at wind speeds of 15 m/s. Using a shroud with a straight flange, the torque is increased by 156.097 percent to 0.315 N.m. The rotational velocity increases by 56.787% to 216.375 rad/s. Also, the power factor reaches 0.568, which indicates an increase of 302.836% compared to the turbine without a shroud. Using the turbine in a shroud with optimal curved flange, the amount of torque, angular velocity, and power factor compared to turbines in a shroud with simple vertical flange configuration has increased by 10.793%, 3.810%, and 15.140%, respectively. By installing a circular vortex generator these percentages will be equal to 14.285%, 7.937%, and 23.415%, respectively.
- The results show that the increase in entropy in the flow through the shroud is very small when a curved flange and a circular vortex generator are installed on the shroud and do not cause significant losses. The largest increase in entropy occurs when a curved flange and a circular vortex generator are used on the shroud, and this increase is only equal to 1.067%, which is a very small amount. Therefore, the use of these tools in the current situation is still very desirable. Efficiency of shroud introduced in the present work has a value equal to 94.8%. This efficiency is a confirmation on the excellent design of the shroud equipped with optimal curved flange and circular vortex generator.
- The limitation of the present work is the selective dimensions of shroud. Due to the fact that in the future, this shroud should be placed in a wind tunnel with a $1 \times 1.2 \times 2$ test chamber, the current dimensions were selected to prevent the phenomenon of blockage.

Declarations

Competing interests

These authors have no competing interests.

References

1. - Ahlborn, Detlef.: Principal component analysis of West European wind power generation. The European Physical Journal Plus. **135**(7), 568 (2020)
2. - Aranake, Aniket C., Vinod K. Lakshminarayan, and Karthik Duraisamy.: Computational analysis of shrouded wind turbine configurations using a 3-dimensional RANS solver. Renewable Energy. **75**, 818–832 (2015). http://dx.doi.org/10.1016/j.renene.2014.10.049

3. - Aranake, A., and K. Duraisamy.: Aerodynamic optimization of shrouded wind turbines. Wind Energy. **20**(5), 877–889 (2017). https://doi.org/10.1002/we.2068
4. - Dilimulati, Aierken, Ted Stathopoulos, and Marius Paraschivoiu.: Wind turbine designs for urban applications: A case study of shrouded diffuser casing for turbines. Journal of Wind Engineering and Industrial Aerodynamics, **175**, 179–192 (2018).https://doi.org/10.1016/j.oceaneng.2020.107252
5. - Shahsavarifard, Mohammad, and Eric Louis Bibeau.: Performance characteristics of shrouded horizontal axis hydrokinetic turbines in yawed conditions. Ocean Engineering. **197**, 106916 (2020).https://doi.org/10.1016/j.oceaneng.2020.106916
6. - Siavash, Nemat Keramat, G. Najafi, Teymour Tavakkoli Hashjin, Barat Ghobadian, and Esmail Mahmoodi.: An innovative variable shroud for micro wind turbines. Renewable Energy. **145**, 1061–1072 (2020). https://doi.org/10.1016/j.renene.2019.06.098
7. - Gish, L. A., A. Carandang, and G. Hawbaker.: Experimental evaluation of a shrouded horizontal axis hydrokinetic turbine with pre-swirl stators. Ocean Engineering. **204**, 107252 (2020).https://doi.org/10.1016/j.jweia.2018.01.003
8. - Han, Wanlong, Peigang Yan, Wanjin Han, and Yurong He.: Design of wind turbines with shroud and lobed ejectors for efficient utilization of low-grade wind energy. Energy. **89**, 687–701 (2015).https://doi.org/10.1016/j.energy.2015.06.024
9. - Kosasih, Buyung, and Andrea Tondelli.: Experimental study of shrouded micro-wind turbine. Procedia Engineering. **49**, 92–98 (2012).https://doi.org/10.1016/j.proeng.2012.10.116
10. - Pambudi, Nugroho Agung, Rusdi Febriyanto, Kukuh Mukti Wibowo, Nova Dany Setyawan, Nyenyep Sri Wardani, Lip Huat Saw, and Bayu Rudiyanto.: The performance of shrouded wind turbine at low wind speed condition. Energy Procedia, **158**, 260–265 (2019).https://doi.org/10.1016/j.egypro.2019.01.086
11. - Leloudas, Stavros N., Georgios N. Lygidakis, Alexandros I. Eskantar, and Ioannis K. Nikolos.: A robust methodology for the design optimization of diffuser augmented wind turbine shrouds. Renewable Energy. **150**, 722–742 (2020).https://doi.org/10.1016/j.renene.2019.12.098
12. - Leloudas, Stavros N., Georgios N. Lygidakis, Giorgos A. Strofylas, and Ioannis K. Nikolos.: Aerodynamic shape optimization of diffuser augmented wind turbine shrouds using asynchronous differential evolution. In ASME International Mechanical Engineering Congress and Exposition, **52101**, V007T09A085 (2018).https://doi.org/10.1115/IMECE2018-86820
13. - Ohya, Yuji, Takashi Karasudani, Akira Sakurai, Ken-ichi Abe, and Masahiro Inoue.: Development of a shrouded wind turbine with a flanged diffuser. Journal of wind engineering and industrial aerodynamics. **96**(5), 524–539 (2008).https://doi.org/10.1016/j.jweia.2008.01.006
14. - Siavash, Nemat Keramat, G. Najafi, Teymour Tavakkoli Hashjin, Barat Ghobadian, and Esmail Mahmoodi.: Mathematical modeling of a horizontal axis shrouded wind turbine. Renewable Energy. **146**, 856–866 (2020).https://doi.org/10.1016/j.renene.2019.07.022
15. - Werle, Michael J.: An enhanced analytical model for airfoil-based shrouded wind turbines. Wind Energy. **23**(8), 1711–1725 (2020). https://doi.org/10.1002/we.2511
16. - Lipian, Michal, Ivan Dobrev, Maciej Karczewski, Fawaz Massouh, and Krzysztof Jozwik.: Small wind turbine augmentation: Experimental investigations of shrouded-and twin-rotor wind turbine systems.

Energy. **186**, 226966 (2019).https://doi.org/10.1016/j.energy.2019.115855

17. - Lipian, Michal, Ivan Dobrev, Fawaz Massouh, and Krzysztof Jozwik.: Small wind turbine augmentation: Numerical investigations of shrouded-and twin-rotor wind turbines. Energy. **201**, 117588 (2020). https://doi.org/10.1016/j.energy.2020.117588
18. - Mamouri, Amir Reza, Abdolamir Bak Khoshnevis, and Esmail Lakzian.: Entropy generation analysis of S825, S822, and SD7062 offshore wind turbine airfoil geometries. Ocean Engineering. **173**, 700–715 (2019).https://doi.org/10.1016/j.oceaneng.2018.12.068
19. - Mamouri, Amir Reza, Abdolamir Bak Khoshnevis, and Esmail Lakzian.: Experimental study of the effective parameters on the offshore wind turbine's airfoil in pitching case. Ocean Engineering. **198**, 106955 (2020).https://doi.org/10.1016/j.oceaneng.2020.106955
20. Niknahad, Ali.: Numerical study and comparison of turbulent parameters of simple, triangular, and circular vortex generators equipped airfoil model. *Journal of Advanced Research in Numerical Heat Transfer.* **8**(1), 1–18 (2022).
21. - Yadegari, Mitra, and Abdolamir Bak Khoshnevis.: Investigation of entropy generation, efficiency, static and ideal pressure recovery coefficient in curved annular diffusers. The European Physical Journal Plus. **136**(1), 1–19 (2021). https://doi.org/10.1140/epjp/s13360-021-01071-1

Figures

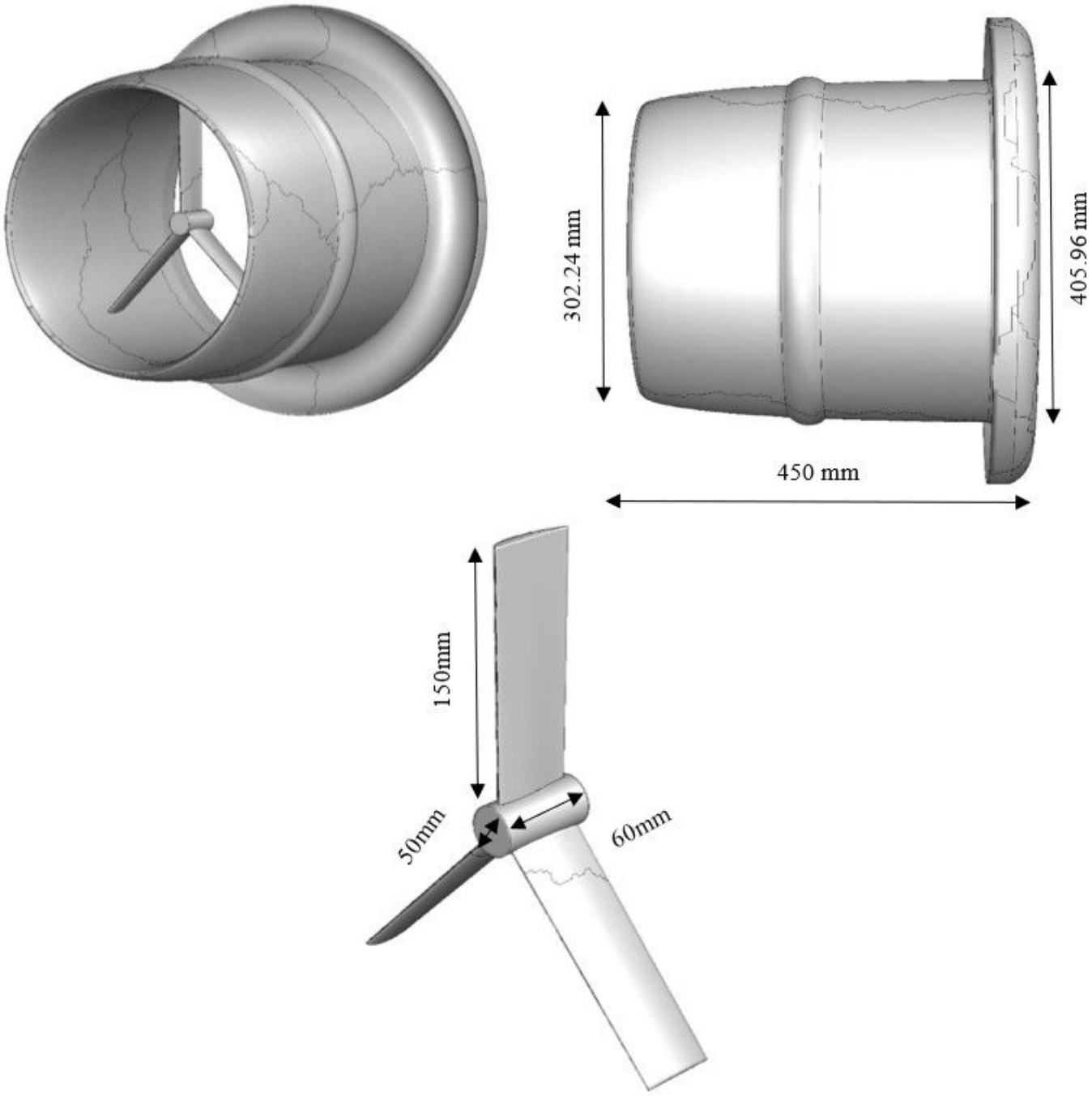

Figure 1

(a) Perspective and (b) side view of a three-dimensional schematic of the shroud and curved flange/vortex generator attached to its end, (c) turbine dimensions

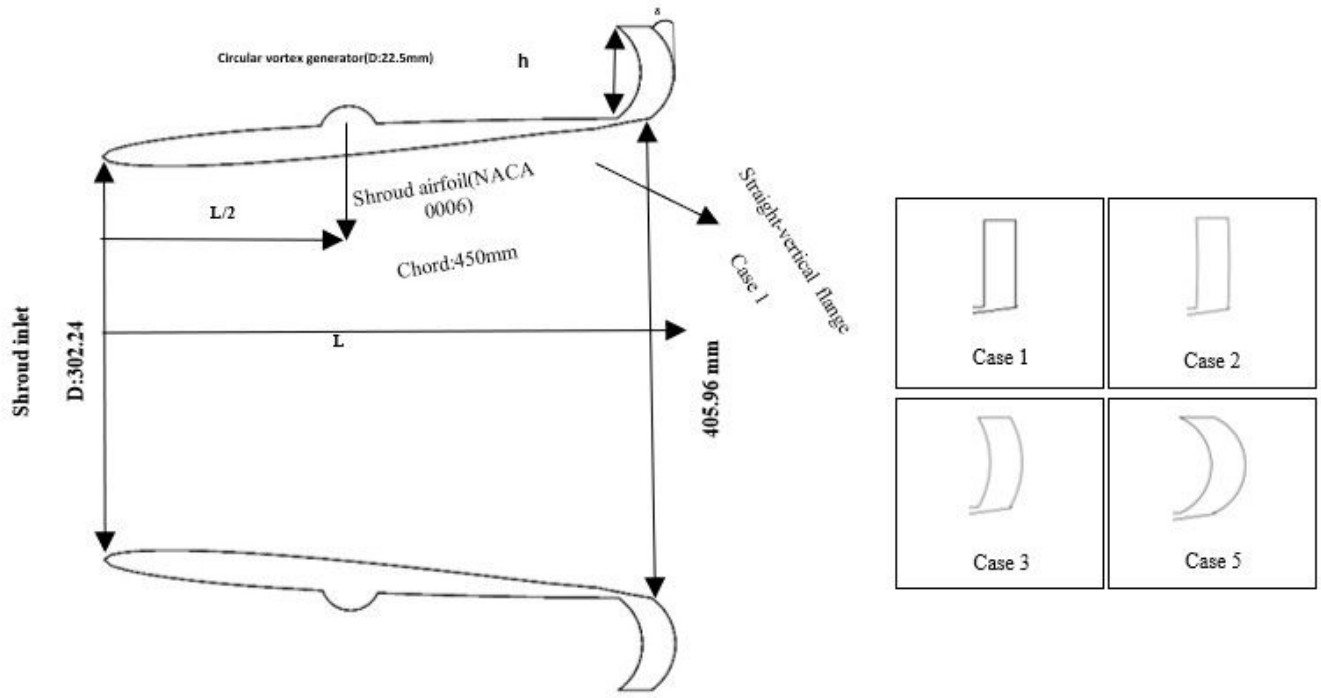

Figure 2

Base shroud model with straight vertical and curved flanges

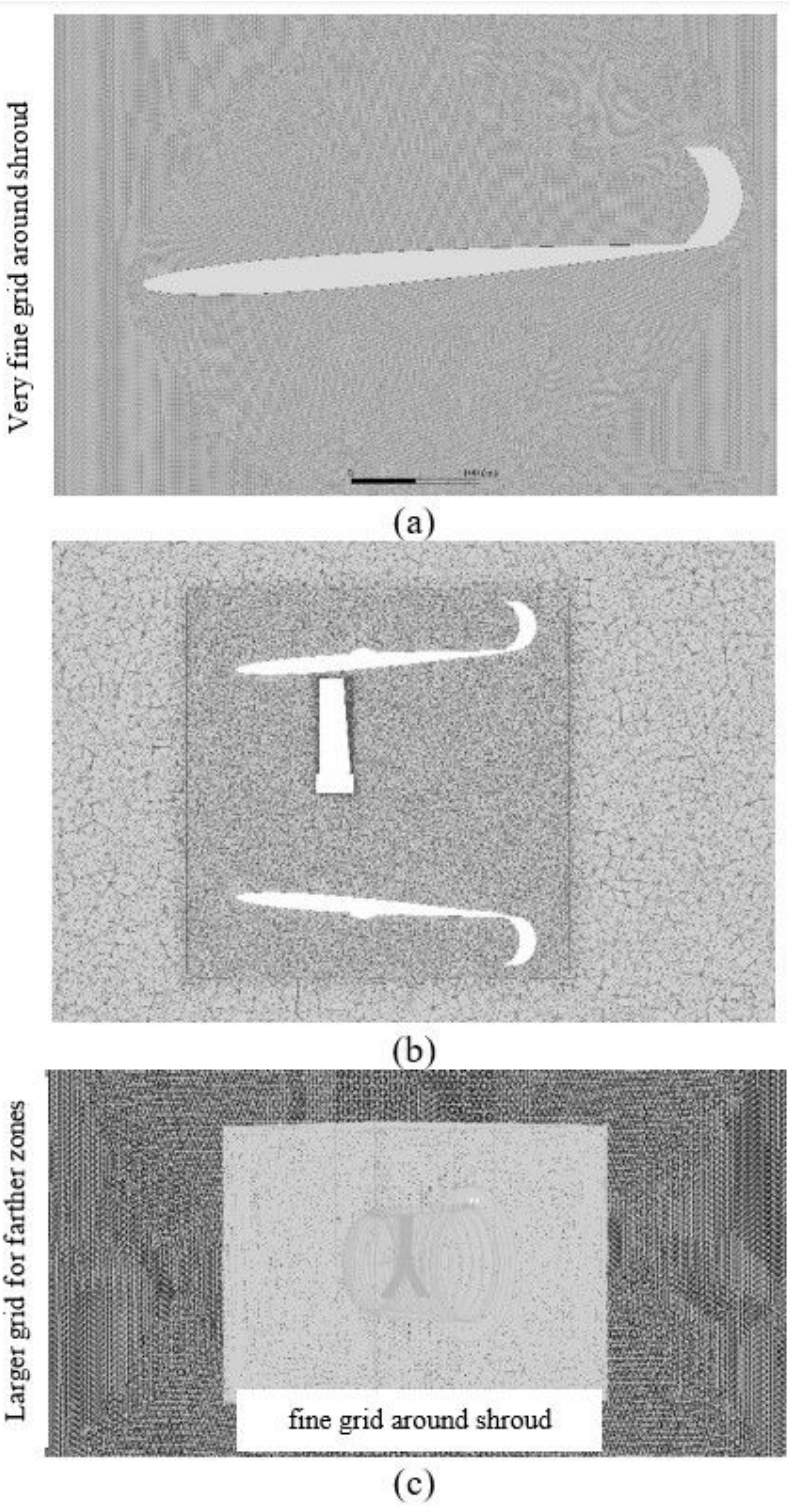

Figure 3

Computational grid around shroud's (a) 2D, (b) and (c) 3D geometries

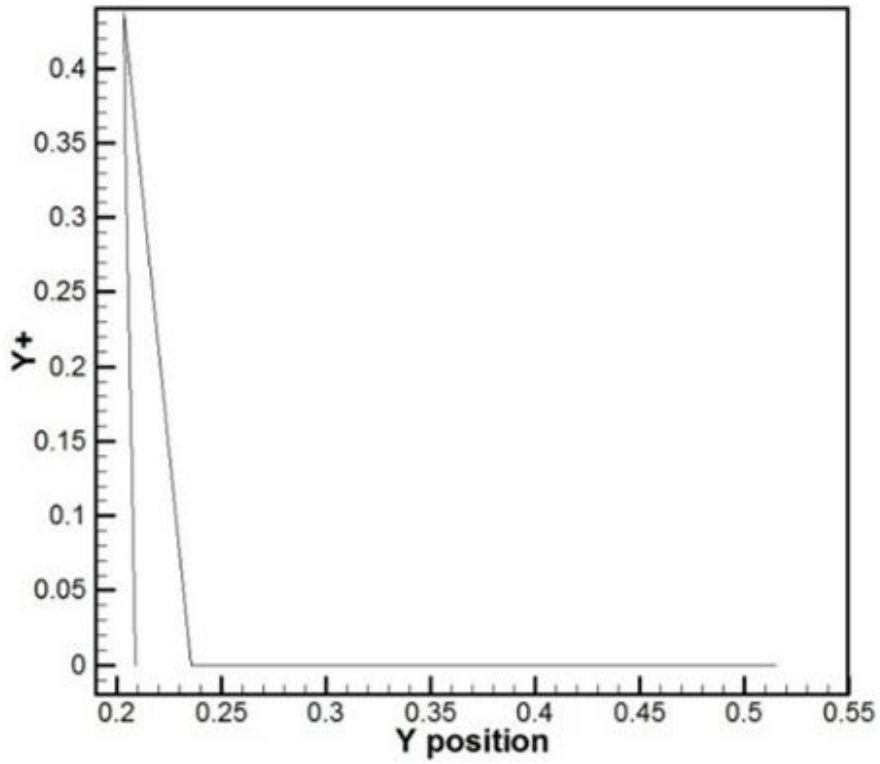

Figure 4

Y Plus changes with the height from the surface of the shroud outer wall

Figure 5

Diffuser-type shroud in the experiment of Ohya et al. [13]

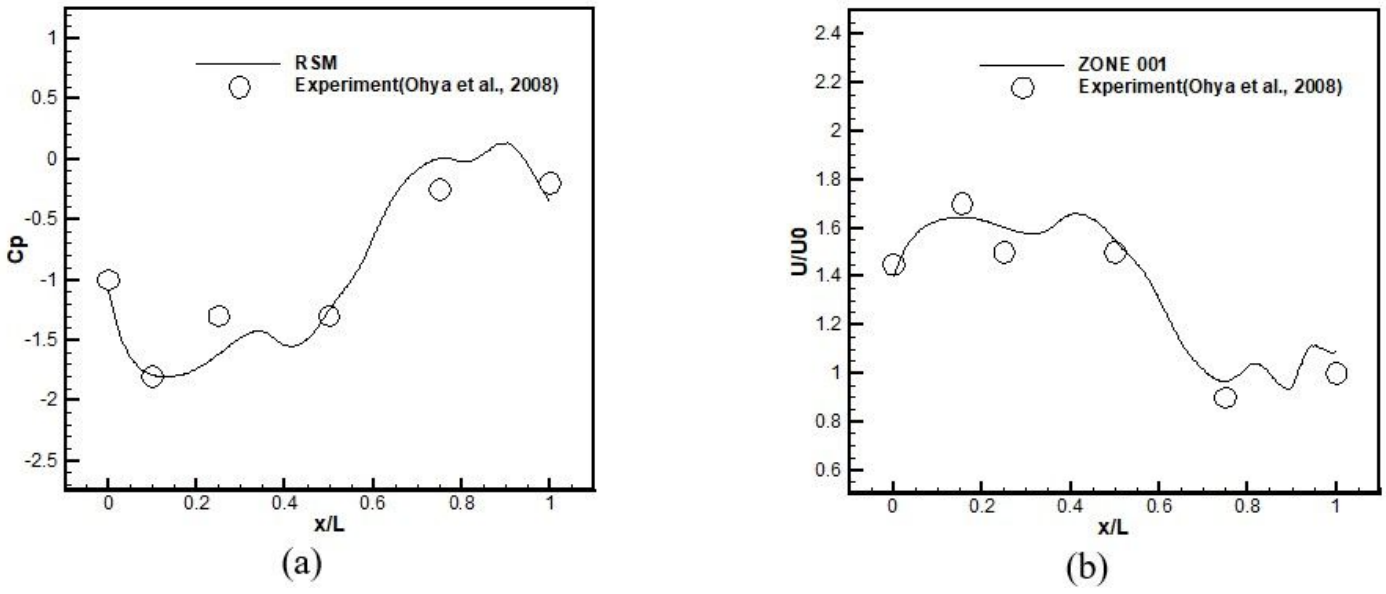

Figure 6

The comparison of (a) Cp and (b) non-dimensional velocity inside the diffuser-type shroud between the experiment of Ohya et al. [13] and the present numerical method

Figure 7

u/U0 profiles at shroud inlet for cases one to five

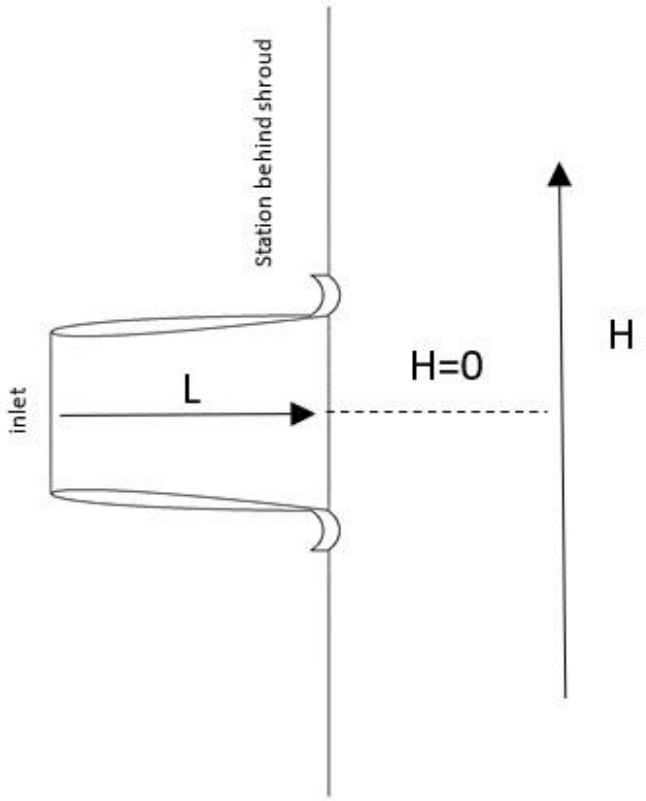

Figure 8

Computational station location behind the shroud

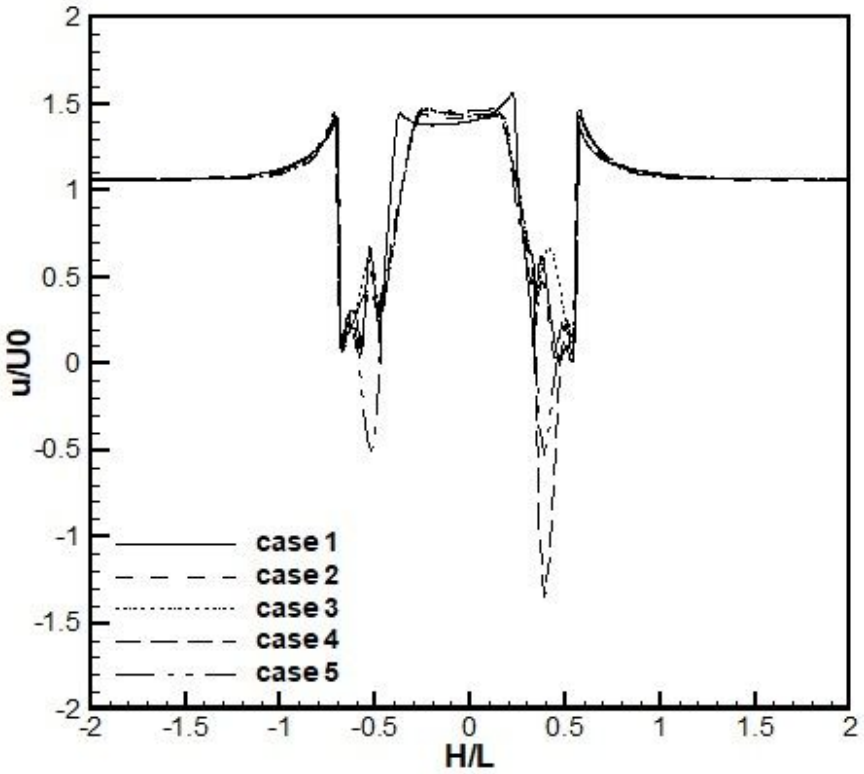

Figure 9

Non-dimensional mean velocity (u /U0) profiles just behind shroud for cases 1 to 5

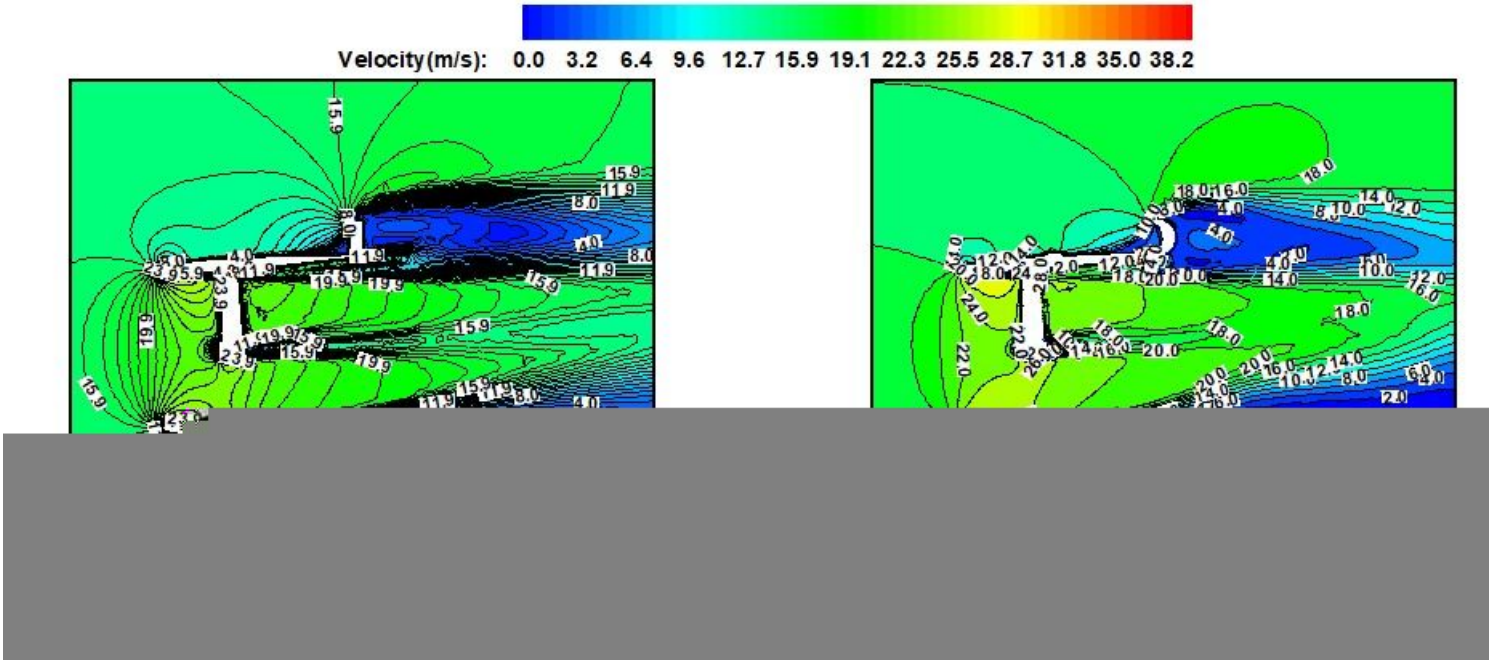

Figure 10

Vortices created by the flange in the side view of the shroud (a) shroud with simple flange, (b) shroud with optimal curved flange and circular vortex generator

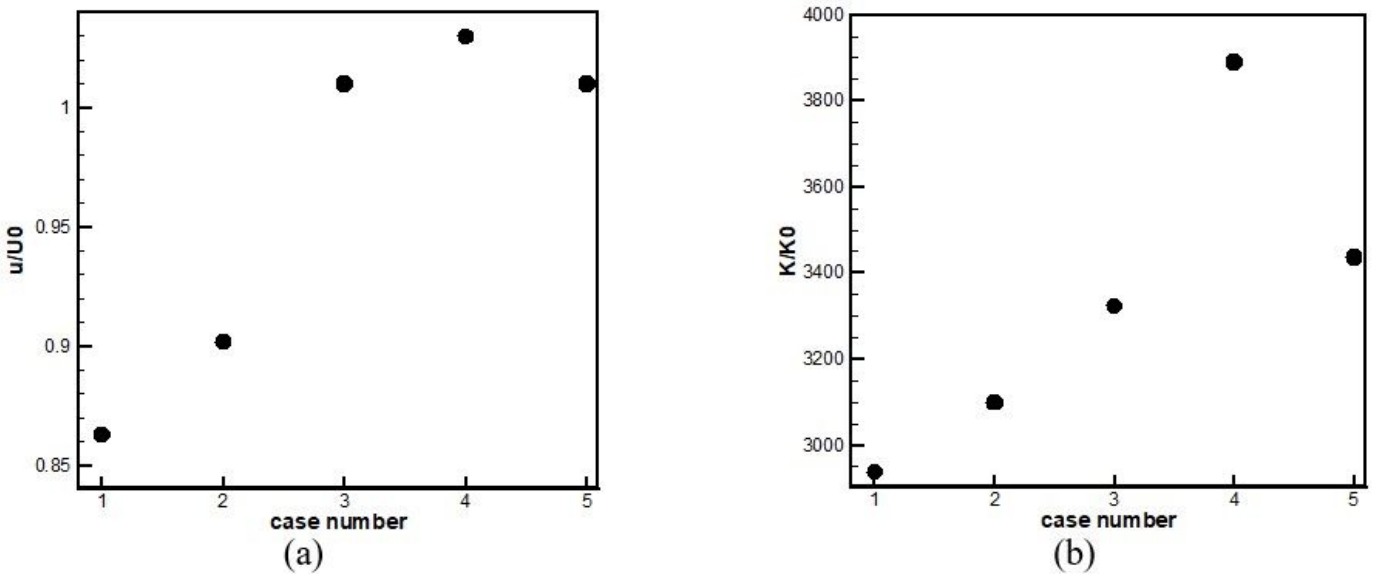

Figure 11

(a) Non-dimensional mean velocity (u/U0) behind shroud for cases 1 to 5, (b) Ratio of average turbulence energy to free-stream turbulence kinetic energy (k/k0) behind shroud for cases 1 to 5

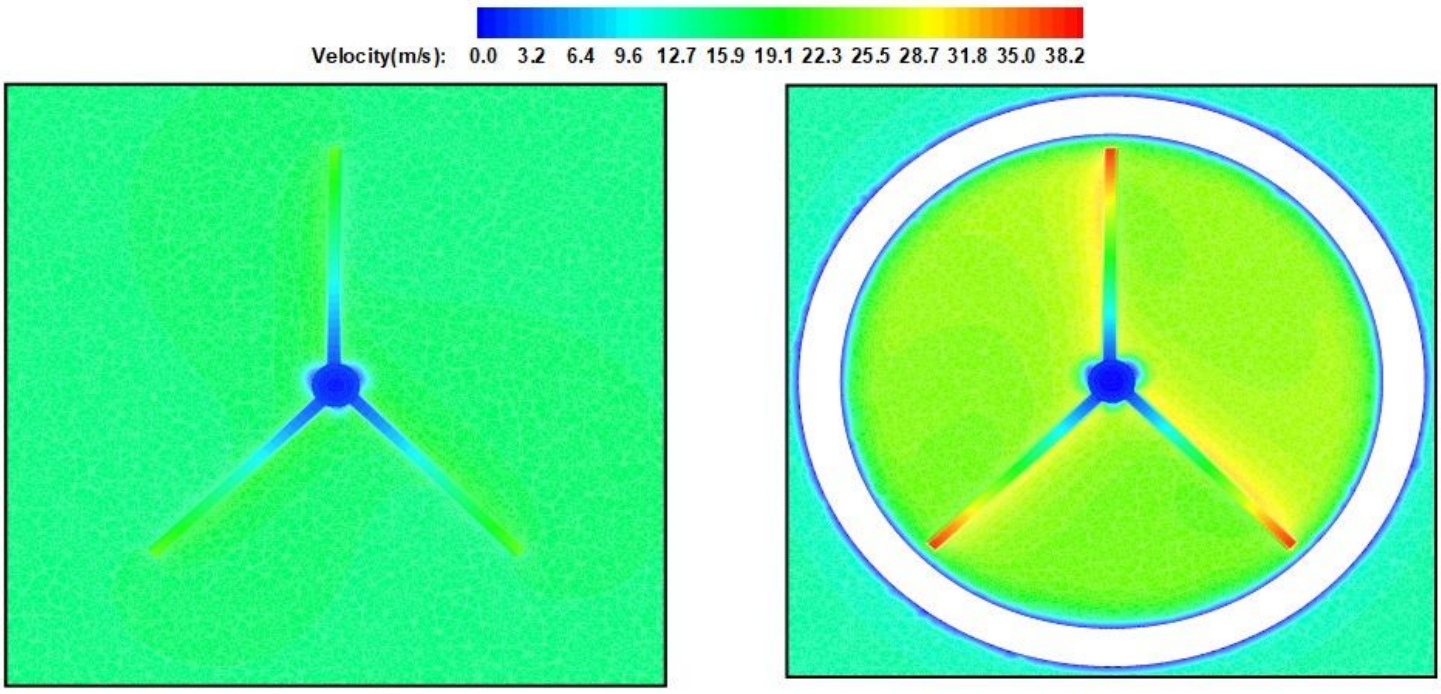

Figure 12

The velocity of the airflow in the turbine section for (a) a turbine without a shroud, (b) a turbine with shroud and a curved flange and a circular vortex generator connected to shroud